Applied Computer Science 2025, vol. 21, no. 4, pp. 21–31
https://doi.org/10.35784/acs_8410

Submitted: 2025-08-27 | Revised: 2025-09-30 | Accepted: 2025-10-13

Keywords: knee osteoarthritis, encoder-based motion analysis, machine learning, vibroarthrography, wearable sensors, knee joint, biomechanics

Robert KARPIŃSKI [1, 2*], *Arkadiusz SYTA* [1]
[1] Lublin University of Technology, Poland, r.karpinski@pollub.pl
[2] The John Paul II Catholic University of Lublin, Poland, r.karpinski@pollub.pl, a.syta@pollub.pl
[*] Corresponding author: r.karpinski@pollub.pl

Application of encoder-based motion analysis and machine learning for knee osteoarthritis detection: A pilot study

Abstract

Osteoarthritis (OA) is the most common joint disease and a leading cause of disability, most commonly affecting the knee. Conventional diagnostics rely primarily on imaging, which often detects changes only in advanced stages. This pilot study explores an alternative approach - encoder-based motion analysis combined with machine learning - to support early functional assessment of knee OA. The study included 90 subjects: 45 patients with radiographic evidence of OA and 45 healthy controls. A high-resolution rotary encoder integrated into a stabilizing knee orthosis recorded joint flexion-extension angles and velocities during open kinetic chain (OKC) and closed kinetic chain (CKC) tasks. Each subject performed five repetitions for each condition. Statistical analyses (Mann-Whitney U-test) revealed significant differences between groups, particularly in the CKC condition, where OA patients consistently required more time to complete movements. Machine learning classifiers were trained on cycle duration features. For OKC, accuracy remained modest (Naive Bayes: 65.6%), whereas CKC-based features provided stronger discrimination, with a narrow neural network achieving 80% accuracy and balanced sensitivity/specificity. The results demonstrate the feasibility of wearable encoder-based systems for objective, non-invasive assessment of knee function. CKC tasks showed higher diagnostic value, highlighting their potential for integration into clinical protocols. Future research should expand data sets, incorporate multimodal sensors, and use advanced algorithms to improve diagnostic performance and support real-world monitoring.

1. INTRODUCTION

Osteoarthritis (OA) is the most common form of arthritis and a leading cause of disability in older adults worldwide (Karpiński et al., 2025a). The condition is characterized by progressive cartilage degradation and degenerative changes throughout the joint, resulting in pain, stiffness, and decreased mobility (Allen et al., 2022; Gelber, 2024). According to the World Health Organization, approximately 528 million people will be affected by OA in 2019 (a 113% increase since 1990), with women accounting for nearly 60% of cases. Current estimates suggest that the disease affects more than 7% of the world's population, and the number of cases continues to rise as populations age (Steinmetz et al., 2023). The knee joint is the most commonly affected, with degenerative changes reported in hundreds of millions of people worldwide (Bryliński et al., 2025; Courties et al., 2024). For example, epidemiologic studies show that nearly 80% of people over the age of 65 have radiographic evidence of OA (Mohammadi et al., 2024). Demographic changes, particularly the aging of the population, along with risk factors such as obesity and mechanical injuries, indicate that the burden of OA will continue to increase in the coming decades (Steinmetz et al., 2023). In advanced stages, when conservative and minimally invasive treatments are no longer effective, joint replacement surgery (arthroplasty) often remains the last therapeutic option for patients with severe OA (Karpiński et al., 2024a, 2024b, 2024c). OA is already recognized as a major factor impairing physical function and quality of life, contributing to substantial social and economic costs (De Tocqueville et al., 2021).

The diagnosis of osteoarthritis is currently based primarily on clinical assessment (history and physical examination) and imaging techniques, most commonly radiography (x-ray), sometimes supplemented by magnetic resonance imaging (MRI) or ultrasound (Karpiński et al., 2025b). However, radiologic features such

as joint space narrowing or osteophyte formation typically appear only in advanced stages of the disease (Mohammadi et al., 2024). Clinical symptoms such as pain, crepitus, and limitation of movement may precede clear radiographic changes, highlighting the need for methods that allow earlier and more sensitive functional assessment of the joints (Karpiński, 2022). Numerical methods, including analytical approaches, Finite Element Method (FEM) calculations, and artificial intelligence algorithms, are widely used in the detailed description of pathological changes in biological structures, enabling a better understanding and prediction of degenerative processes, as well as the development of hybrid diagnostic tools to aid in clinical assessment and early disease detection (Matthews et al., 2020; Sbriglio et al., 2025; Zalzal et al., 2004).

In recent years, there has been a growing interest in vibroacoustic diagnostics of joints, also known as vibroarthrography (VAG). In particular, vibroacoustic diagnostics originated in mechanical engineering, where it was widely used to evaluate the technical condition of machines and devices through the analysis of vibrations and noise (Jedliński et al., 2022; Jedliński & Jonak, 2017; Litak et al., 2010). Over time, these methods have been adapted for biomedical applications, allowing them to be used to assess the function of the human musculoskeletal system, particularly the knee joints (Kręcisz, 2023; Łysiak et al., 2025; Machrowska et al., 2024a).

In this method, vibrations and sounds generated by the joint during movement (knee flexion and extension) are recorded using sensors attached to the skin directly over the joint being examined (Bączkowicz & Majorczyk, 2014; Cai et al., 2013; Machrowska et al., 2025). More than a century ago, auscultation of the knee joint was described as a means of detecting abnormalities, and today the technique has advanced through the use of piezoelectric sensors and high-sensitivity accelerometers (Befrui et al., 2018; Rangayyan et al., 1997; Shark et al., 2011; Tanaka & Hoshiyama, 2012; Whittingslow et al., 2020). Research has shown that knees affected by degenerative changes produce acoustic signals of greater amplitude and longer duration during movement compared to healthy joints (Krakowski et al., 2021; Machrowska, 2024b; Wu et al., 2016). Cartilage degeneration and increased intra-articular friction result in characteristic vibrations that can be recorded and analyzed. Importantly, vibroacoustic diagnostics are non-invasive, rapid, repeatable, and free of radiation exposure, while providing information on the dynamic function of the joint that cannot be captured by static MRI or radiographic images (Karpiński et al., 2025b; Khokhlova et al., 2021). Reports in the literature are promising, with preliminary preclinical studies indicating that the accuracy of this method in detecting cartilage defects exceeds 90% (Rangayyan & Wu, 2009; Wang et al., 2021). However, despite the development of numerous prototype systems, vibroacoustic diagnostics is not yet clinically standardized. Ongoing work focuses on optimizing sensor placement, measurement protocols, and signal processing techniques to minimize artifacts and inter-individual variability.

In light of these advances, a promising research direction is to combine innovative wearable sensors with advanced signal analysis and machine learning techniques. This study presents an original experimental approach to the diagnosis of knee osteoarthritis using data acquired from an encoder integrated into the rotational axis of a knee brace. The encoder allows precise measurement of knee joint angles and velocities during flexion and extension under dynamic conditions. The underlying assumption is that analysis of such motion signals can reveal subtle abnormalities in joint function - such as increased resistance, micro-vibrations, or altered motion fluidity - that reflect early cartilage damage and structural joint changes. Incorporating an encoder into an orthosis also opens the possibility of continuous, real-world monitoring of joint performance, providing in vivo functional information that cannot be obtained from a single imaging study. This article outlines the global context of OA, reviews the current state of knowledge on vibroacoustic diagnostics and machine learning applications, and introduces the concept of using orthotic encoder signals to detect degenerative changes. The aim of the study is to evaluate the feasibility and diagnostic potential of this approach and to determine whether knee motion parameters recorded by a sensor-equipped orthosis can serve as valuable digital biomarkers of knee osteoarthritis.

2. MATERIALS AND METHODS

Within the framework of cooperation between the Lublin University of Technology, the Independent Public Health Center in Łęczna and the Medical University of Lublin, experimental research was conducted to collect the data analyzed in this study. The primary data set was obtained from workplace investigations using a proprietary measurement system, conducted both in the orthopedic ward and in the laboratory facilities of the Lublin University of Technology.

2.1. Study participants

The study group consisted of 90 subjects: 45 patients with knee osteoarthritis (OA) and 45 healthy volunteers (HC). Patients with OA had radiographic and clinical evidence of advanced degenerative changes in the knee joint and were scheduled for surgical treatment (e.g., arthroscopy or endoprosthetic implantation). Control subjects reported no history of knee pain or injury.

The mean age of the OA patients was 56.1 ± 14.9 years, which was significantly higher than that of the control group (29.3 ± 12.6 years). Body weight and BMI were also higher in the OA group (85.5 ± 16.7 kg; BMI 29.3 ± 3.7) compared to the HC group (67.4 ± 15.1 kg; BMI 20.9 ± 5.0). The control group was predominantly female (29 females, 16 males), whereas the OA group had a balanced gender distribution (24 females, 21 males).

In the present study, all patients included in the OA group had radiographically and clinically confirmed knee osteoarthritis, with disease severity classified according to the Kellgren–Lawrence (K–L) grading system (Kohn et al., 2016; Olsson et al., 2021), most frequently grades III–IV. The K–L system distinguishes four main stages: grade I (doubtful OA – minimal osteophytes, no joint space narrowing), grade II (mild OA – definite osteophytes, possible joint space narrowing), grade III (moderate OA – multiple osteophytes, definite joint space narrowing, possible subchondral sclerosis), and grade IV (severe OA – large osteophytes, marked joint space narrowing, severe sclerosis, and possible bone deformity). Intraoperative assessment further confirmed advanced degenerative changes and cartilage damage, which were additionally categorized using the Outerbridge classification (Slattery & Kweon, 2018). This dual grading approach ensured a reliable and reproducible definition of disease stage in the OA cohort.

It should be emphasized that the osteoarthritis (OA) and healthy control (HC) groups differed significantly in terms of age, BMI, and sex distribution. However, these differences reflect the natural clinical characteristics of knee osteoarthritis, which predominantly affects individuals over the age of 50. The inclusion of younger volunteers in the control group was intended to minimize the risk of asymptomatic cartilage lesions, which are common in older populations. Full matching with respect to age and body weight was not feasible due to clinical eligibility criteria for surgical treatment and organizational constraints (including those related to the COVID-19 pandemic).

Both groups nevertheless underwent a comprehensive clinical and orthopedic evaluation, and in the OA group the presence of cartilage damage was intraoperatively confirmed and classified according to the Outerbridge grading system, thereby strengthening the reliability of group assignment. Although demographic differences may represent a potential confounding factor, the adopted measurement protocol—covering the full range of knee motion—helped to mitigate their impact on signal analysis. Future studies will include better age-, BMI-, and sex-matched control groups to further minimize the risk of confounding effects.

All participants were fully informed about the study's objectives, procedures, and potential risks, and provided written informed consent. The study protocol was approved by the Bioethics Committee of the Medical University of Lublin (No. KE-0254/261/2019) and conducted in accordance with the principles of Good Clinical Practice. Additionally, each participant underwent a standard clinical examination of the knee joint, and knee function was assessed using the Lysholm questionnaire. The results in the OA group (mean ~45 points) indicated significant functional impairment, whereas healthy individuals achieved nearly maximum values (mean ~95 points).

2.2. Measurement system and test protocol

The knee mobility measurement station was based on a digital rotary encoder. A high-precision encoder (EMS22A50, Bourns) with a resolution of 1024 pulses per revolution was integrated into the axis of the stabilizing knee brace, allowing continuous measurement of joint flexion angles and calculation of angular velocity during motion. The signals were recorded with a sampling frequency of 1400 Hz and a resolution of 10 bits, ensuring sufficient temporal resolution and accuracy in mapping the knee kinematics. The orthosis provided both stabilization and structural support for the sensor, ensuring repeatability and safety of the measurements.

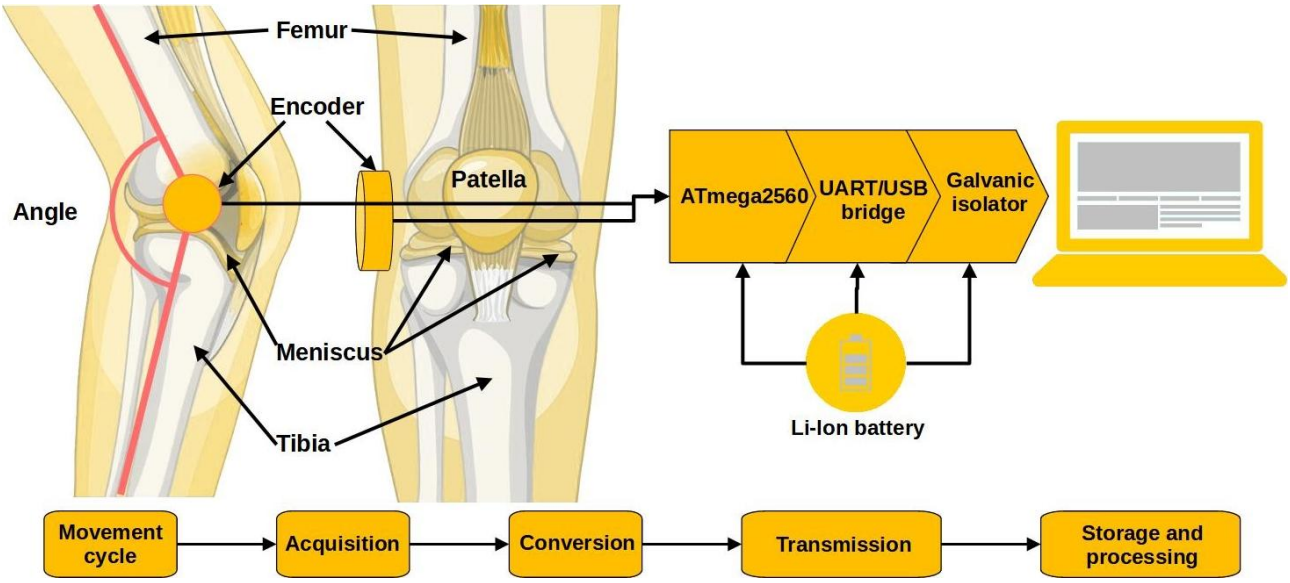

Fig. 1. Block diagram of the measurement system

Signals from the encoder were transmitted to a measurement card connected to a PC equipped with dedicated software for real-time data acquisition and processing. The complete measurement system is presented in Fig. 1, which shows, in sequence: the tested joint with the brace and encoder, the signal acquisition track, the measurement card, and the computer unit.

The protocol involved active knee extension and flexion within a range of 90° to 0° and back, performed under both open kinetic chain (OKC) and closed kinetic chain (CKC) conditions. In OKC, participants sat with the lower limb hanging freely and executed extension from 90° to 0°, followed by flexion back to 90°. In CKC, participants performed a sit-to-stand movement (knee flexion from approximately 90° to 0°) and then returned to sitting, with feet firmly supported on the ground. Each participant completed five repetitions of both movement variants, maintaining a consistent pace of ~2 seconds per full cycle, which ensured repeatable and comparable recordings.

2.3. Statistical analysis and machine learning approach

Statistical analyses were performed to compare task completion times between the healthy control (HC) and osteoarthritis (OA) groups. For each test condition (open chain, OKC; closed chain, CKC) and each of the five cycles, between-group comparisons were made using the nonparametric Mann-Whitney U test. This test was chosen because it does not assume normally distributed data and is appropriate for independent samples. A significance level of $\alpha = 0.05$ was used. In addition to the descriptive statistics (box plots), detailed results of the statistical comparisons are presented in Tables 1 and 2.

In addition to statistical testing, the measured durations of individual cycles were pre-processed and formatted into an input dataset for machine learning models. The goal was to perform a binary classification (HC vs. OA) based on the test performance. The training process used a 5-fold cross-validation scheme to ensure robust evaluation of model performance and to minimize the risk of overfitting.

Six classifiers available in the MATLAB Classification Learner Toolbox were used in this study. Each model represents a different family of machine learning methods, allowing the data to be analyzed from different methodological perspectives.

The first algorithm used was Naive Bayes, a probabilistic classifier based on Bayes' theorem that assumes conditional independence of input features. Due to its simplicity and computational efficiency, Naive Bayes is widely used in text classification and tabular data analysis (Machrowska et al., 2020a; Messaoudene & Harrar, 2022; Mitchell, 2013; Szabelski et al., 2022).

The second model was k-Nearest Neighbors (KNN), an instance-based learning algorithm that assigns a class label according to the majority vote of the k nearest neighbors in the feature space. While intuitive and nonparametric, KNN can be sensitive to redundant features and noise (Cover & Hart, 1967; Kulisz, et al., 2024; Machrowska et al., 2020b).

Another classifier used in the experiments was the Support Vector Machine (SVM). This method constructs a hyperplane that maximizes the margin of separation between classes. Due to its margin-maximization principle, SVM performs effectively in both linear and nonlinear classification tasks, especially in high-dimensional spaces (Cortes & Vapnik, 1995; Falkowicz & Kulisz, 2024).

The study also applied logistic regression (GLM), which is a special case of generalized linear model with logit link function and Bernoulli distribution. Logistic regression is a classical statistical method that is widely used for both binary and multiclass classification (Hosmer et al., 2013).

In addition, two neural network architectures available in the Classification Learner Toolbox were used: Narrow Neural Network and Wide Neural Network. Both models are feedforward multilayer perceptrons with a single hidden layer, differing in the number of hidden neurons - narrow networks use a relatively small number (e.g. 10), while wide networks use significantly more (e.g. 100). The broader architecture allows for greater capacity to approximate nonlinear patterns in the data, but increases the risk of overfitting (Bishop, 1995; Goodfellow et al., 2016; Kulisz et al., 2024; Kulisz, et al., 2024; Kwiatkowski et al., 2023).

3. RESULTS

The duration of 5 repetition cycles (analyzed as single cycles) was examined and compared for each participant in both tests, in the control group (45 individuals) and in the patient group (45 individuals). This approach primarily allowed us to assess the stability of the repetition dynamics over time and to compare them between groups and test types. Figure 2 shows a graphical summary of the basic statistics (box plots) for the individual cycles and sequences.

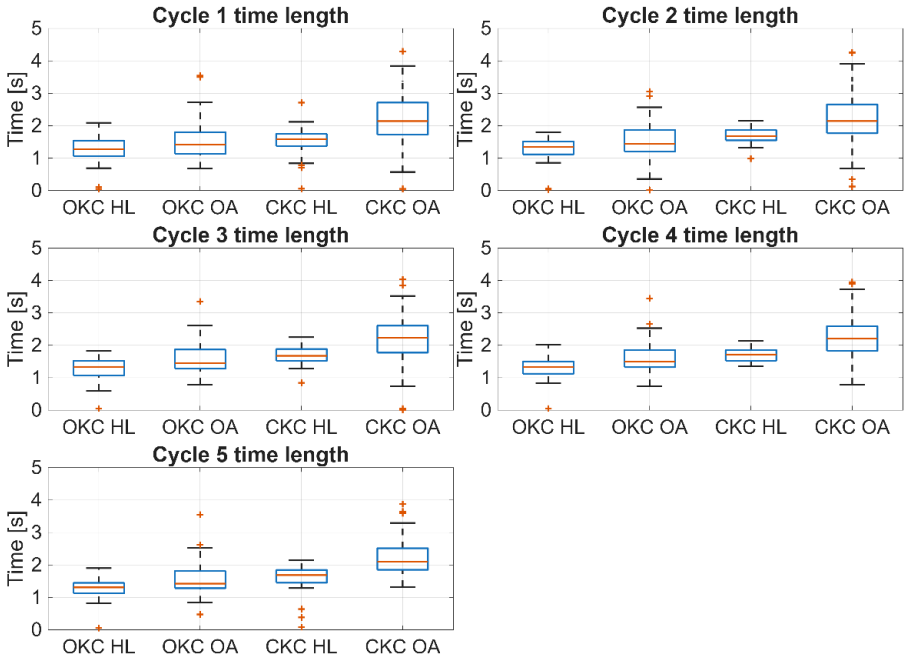

Fig. 2. Statistical comparison of the duration of individual cycles

Analysis of the box plots comparing the duration of each cycle indicates that the results are stable and repeatable over time. As expected, participants in the control group (HC) completed each repetition faster in both tests (OKC and CKC) compared to the osteoarthritis group (OA). The differences between the two test types were generally consistent across the test scenarios, with the largest discrepancies observed in the closed chain condition. This may be explained by the increased biomechanical demands and greater load transfer through the affected joints during closed-chain tasks, which may disproportionately slow performance in patients with osteoarthritis. We compared task completion time between healthy controls (HC) and patients with osteoarthritis (OA) using the nonparametric Mann-Whitney U test (also known as the Wilcoxon rank-

sum test). The results of the statistical analyses for the open chain (OKC) and closed chain (CKC) conditions are shown in Tables Tab. 1 and Tab. 2, respectively.

Tab. 1. Open-Chain Kinematic Test (OKC) – comparison of cycle durations

Cycle	Comparison	N (HC)	N (OA)	Mean HC (s)	Mean OA (s)	Mean Diff (s)	p-value	Significant
Cycle 1	HC vs OA	45	45	1.246	1.528	-0.283	0.0688	No
Cycle 2	HC vs OA	45	45	1.297	1.501	-0.204	0.1005	No
Cycle 3	HC vs OA	45	45	1.302	1.607	-0.305	0.0070	Yes
Cycle 4	HC vs OA	45	45	1.305	1.589	-0.284	0.0044	Yes
Cycle 5	HC vs OA	45	45	1.292	1.563	-0.272	0.0062	Yes

Tab. 2. Close-Chain Kinematic Test (CKC) – comparison of cycle durations.

Cycle	Comparison	N (HC)	N (OA)	Mean HC (s)	Mean OA (s)	Mean Diff (s)	p-value	Significant
Cycle 1	HC vs OA	45	45	1.514	2.211	-0.697	3.91e-06	Yes
Cycle 2	HC vs OA	45	45	1.691	2.211	-0.520	3.07e-05	Yes
Cycle 3	HC vs OA	45	45	1.695	2.202	-0.507	3.42e-05	Yes
Cycle 4	HC vs OA	45	45	1.695	2.252	-0.556	1.78e-06	Yes
Cycle 5	HC vs OA	45	45	1.610	2.225	-0.616	2.21e-07	Yes

In the open-chain condition, the mean completion time was consistently lower in the healthy control group (HC) compared with the osteoarthritis group (OA). However, the differences between groups were not statistically significant in the first two cycles ($p = 0.069$ and $p = 0.101$, respectively; Tab.1). From the third cycle onward, significant group differences were observed, with HC completing the repetitions faster than OA (p-values ranging from 0.004 to 0.007). These findings suggest that performance disparities between groups become more evident over time, indicating that the open-chain condition may reveal cumulative differences in motor control and endurance. In the closed-chain condition, the differences between groups were more consistent and robust (Tab.2). Across all five cycles, HC participants performed significantly faster than OA participants, with mean differences ranging from –0.51 to –0.70 seconds (all $p < 0.001$). These results indicate stable and reproducible performance across cycles and highlight that patients with osteoarthritis experience consistently longer execution times under the closed-chain condition compared with healthy controls. The greater biomechanical load and higher joint demands in closed-chain movements likely contribute to the observed performance gap.

Using the cycle duration data as input features, several machine learning classifiers were trained in MATLAB R2025a to distinguish between healthy controls (HC) and osteoarthritis patients (OA). Model performance was evaluated using a 5-fold cross-validation procedure. The three best-performing classifiers for each test condition (OKC and CKC) are summarized in tables Tab. 3 and Tab.4 respectively. For each classifier, key performance metrics (accuracy, sensitivity, specificity, and F1-score) are reported.

Tab. 3. Classification results for OKC condition (5-fold cross-validation, MATLAB R2025a)

Classifier	Accuracy (%)	Macro Precision (%)	Macro Recall (%)	Macro F1-score (%)
Naive Bayes	65.6	69.9	65.6	63.6
KNN	65.6	67.5	65.6	64.6
SVM	63.3	67.0	63.3	61.2

Tab. 4. Classification results for CKC condition (5-fold cross-validation, MATLAB R2025a)

Classifier	Accuracy (%)	Macro Precision (%)	Macro Recall (%)	Macro F1-score (%)
Narrow Neural Network	80.0	80.0	80.0	80.0
Logistic Regression (GLM)	77.8	78.3	77.8	77.7
Wide Neural Network	77.8	77.8	77.8	77.8

In the open chain condition (OKC), classification based on cycle duration features achieved moderate accuracy across models (Table 3). The best performance was obtained using a Naive Bayes classifier with an accuracy of 65.6%, macro precision of 69.9%, macro recall of 65.6% and macro F1 score of 63.6%. Similar

results were obtained with the K-Nearest Neighbors (KNN) classifier, while the Support Vector Machine (SVM) performed slightly worse with an accuracy of 63.3% and a macro F1-score of 61.2%.

These results indicate that although the models were able to capture differences between HC and OA participants in the OKC condition, classification accuracy remained modest, suggesting that the discriminative power of open-chain performance measures alone is limited.

In the closed-chain condition (CKC), machine learning classifiers showed significantly higher performance than in the open-chain setting (Table 4). The best results were obtained with a narrow neural network, which achieved 80% accuracy, macro precision, recall and F1 score, reflecting a balanced classification between HC and OA groups. Logistic regression (GLM) and a wide neural network model yielded slightly lower but comparable performance (accuracy ~77.8%).

Overall, these results indicate that cycle duration features from the CKC condition have stronger discriminative power for distinguishing HC from OA than those from the OKC condition, confirming the higher sensitivity of the closed-chain test to group differences.

To further illustrate the classification performance, confusion matrices were generated for the best model in each condition (OKC and CKC), as shown in Figure 3. These matrices provide a detailed overview of true positive, true negative, false positive, and false negative classifications, highlighting the ability of the models to correctly identify group membership.

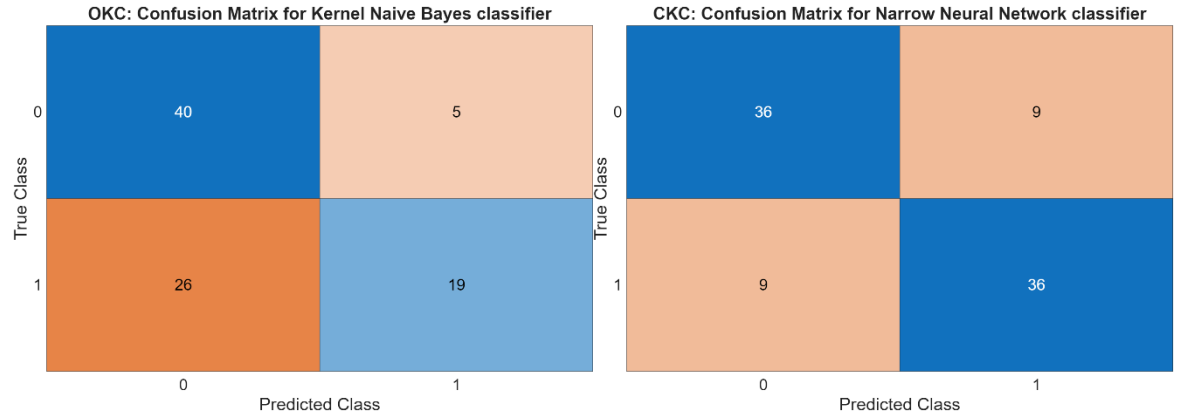

Fig. 3. Confusion matrices for the best-performing classifiers in the open-chain (OKC, left) and closed-chain (CKC, right) conditions

In the OKC condition (Naive Bayes classifier), the model correctly identified 40 HC subjects and 19 OA subjects. However, misclassification was frequent in the OA group, with 26 OA subjects misclassified as HC, which lowered the overall sensitivity for detecting OA cases.

In contrast, the CKC condition (neural network classifier) showed a more balanced classification performance, with 36 correctly identified HC and 36 correctly identified OA subjects. Only 9 subjects from each group were misclassified, resulting in higher accuracy and more stable performance across classes.

Overall, the confusion matrices confirm that CKC features provide greater discriminative power and lead to more reliable classification between HC and OA compared to OKC features, where OA subjects were more often misclassified.

4. DISCUSSION

Statistical analyses confirmed significant differences in task completion times between healthy controls (HC) and patients with osteoarthritis (OA). In the OKC condition, the differences between groups were less consistent: no significant effects were observed in the first two cycles, whereas cycles three to five showed clear differences between groups. This suggests that open-chain tasks may only partially capture functional impairments in OA, becoming more sensitive as the test progresses and fatigue or reduced endurance manifests. In contrast, the CKC condition consistently showed highly significant differences across all five cycles, with OA participants taking significantly more time to complete the tasks. This suggests that closed-loop movements, which involve greater biomechanical stress and more complex neuromuscular control, provide a more robust measure of functional impairment.

Machine learning results support these findings. Classification based on OKC features achieved only moderate accuracy, with a tendency to misclassify OA participants as healthy controls, reflecting the weaker discriminative signal in open-chain tasks. In contrast, classifiers trained on CKC features achieved significantly higher accuracy and more balanced performance, as demonstrated by the confusion matrices. The superior discriminative power of the CKC features is likely due to the higher mechanical demands and joint loading associated with closed chain conditions, which exacerbate the performance gap between OA patients and healthy individuals.

Taken together, both the statistical and machine learning analyses indicate that the CKC state is a more reliable and clinically meaningful test for detecting functional impairment in osteoarthritis. These findings suggest that incorporating closed-loop assessments into clinical evaluation protocols could improve diagnostic accuracy and provide a stronger foundation for machine learning-based decision support systems.

Recent advances have applied machine learning and deep learning to biomechanical gait data for OA assessment, demonstrating high accuracy in early detection of knee osteoarthritis (KOA) (Bandara et al., 2025; McPherson et al., 2024; Wipperman et al., 2024). For example, markerless vision-based approaches have significantly improved KOA classification from gait kinematics, and reviews note that the integration of computational models with wearable sensor data and ML holds great promise for understanding the biomechanics of OA (Ben Hassine et al., 2024; Diamond et al., 2024). These methods typically use detailed biomechanical characteristics, parameters such as swing phase angular velocity or jerk-based smoothness indices, which are sensitive to subtle joint changes even in early OA (Bandara et al., 2025; Castro Mejia et al., 2024).

5. LIMITATIONS AND FUTURE PLANS

This pilot study has several limitations that should be acknowledged. First, the relatively small sample size and the inclusion of patients with advanced stages of knee osteoarthritis may limit the generalizability of the findings to earlier disease stages. Second, the encoder-based measurement system focused primarily on movement duration and angular velocity, without incorporating additional biomechanical or physiological parameters such as ground reaction forces, electromyography (EMG), or pain-related functional scales, which could provide a more comprehensive assessment. An additional limitation is the imbalance in age, BMI, and sex distribution between OA and HC groups, which may have partially influenced the observed differences. Future research should therefore prioritize recruitment of more demographically matched cohorts to strengthen the robustness and generalizability of the findings. Moreover, the machine learning models were trained on a limited feature set derived from cycle durations, which, while informative, may not fully capture the complexity of joint kinematics. Finally, as data collection was performed in controlled laboratory and clinical settings, it remains uncertain how well this approach will translate to continuous monitoring under real-world conditions.

Future work will focus on expanding the participant pool to include individuals at different stages of knee osteoarthritis, as well as at-risk populations, to evaluate the method's diagnostic sensitivity across disease progression. The integration of multimodal sensor data—combining encoders with inertial measurement units (IMUs), EMG, or acoustic sensors—will allow for richer biomechanical characterization and more robust machine learning models. Additionally, advanced algorithms such as deep learning and ensemble methods will be explored to improve classification accuracy and generalizability. A long-term goal is to develop a clinically validated, wearable smart orthosis capable of real-time, at-home monitoring, thereby supporting early detection, personalized treatment planning, and rehabilitation progress tracking in patients with knee osteoarthritis.

6. CONCLUSIONS

This pilot study demonstrated that encoder-based motion analysis combined with machine learning offers a promising approach for functional assessment of knee osteoarthritis. The results confirmed that closed-chain (CKC) tasks provided more robust differentiation between healthy controls and OA patients compared with open-chain (OKC) movements, both in statistical analyses and in classification performance. Machine learning models trained on CKC-derived features achieved accuracy levels up to 80%, indicating the diagnostic potential of this approach.

These findings highlight the feasibility of integrating wearable encoder-based systems into clinical and rehabilitation practice. Such solutions may support early diagnosis, personalized treatment planning, and long-term monitoring of joint function. However, the encoder signal alone is not sufficient for precise diagnosis and should be regarded as an auxiliary source of information. It can serve as an additional feature input for machine learning models, complementing other biomechanical or clinical data.

Further research with larger and more diverse cohorts, enriched sensor modalities, and advanced computational methods is warranted to validate and extend the clinical applicability of this method.

ABBREVIATIONS

BMI – Body Mass Index
CKC – Closed Kinetic Chain
EMG – Electromyography
GLM – Generalized Linear Model
HC – Healthy Control
IMU – Inertial Measurement Unit
KNN – k-Nearest Neighbors
KOA – Knee Osteoarthritis
ML – Machine Learning
MRI – Magnetic Resonance Imaging
OA – Osteoarthritis
OKC – Open Kinetic Chain
PC – Personal Computer
SVM – Support Vector Machine
VAG – Vibroarthrography

Conflicts of interest

The authors declare no conflict of interest.

REFERENCES

Allen, K. D., Thoma, L. M., & Golightly, Y. M. (2022). Epidemiology of osteoarthritis. *Osteoarthritis and Cartilage*, *30*(2), 184–195. https://doi.org/10.1016/j.joca.2021.04.020

Bączkowicz, D., & Majorczyk, E. (2014). Joint motion quality in vibroacoustic signal analysis for patients with patellofemoral joint disorders. *BMC Musculoskeletal Disorders*, *15*, 426. https://doi.org/10.1186/1471-2474-15-426

Bandara, A., Shimizu, H., Watanabe, D., Misa, T., Suzuki, S., Tanigawa, K., Nagai-Tanima, M., & Aoyama, T. (2025). Diurnal variations in gait parameters among older adults with early-stage knee osteoarthritis: Insights from wearable sensor technology. *Scientific Reports*, *15*, 8026. https://doi.org/10.1038/s41598-025-91617-5

Befrui, N., Elsner, J., Flesser, A., Huvanandana, J., Jarrousse, O., Le, T. N., Müller, M., Schulze, W. H. W., Taing, S., & Weidert, S. (2018). Vibroarthrography for early detection of knee osteoarthritis using normalized frequency features. *Medical & Biological Engineering & Computing*, *56*(8), 1499–1514. https://doi.org/10.1007/s11517-018-1785-4

Ben Hassine, S., Balti, A., Abid, S., Ben Khelifa, M. M., & Sayadi, M. (2024). Markerless vision-based knee osteoarthritis classification using machine learning and gait videos. *Frontiers in Signal Processing*, *4*, 1479244. https://doi.org/10.3389/frsip.2024.1479244

Bishop, C. M. (1995). *Neural Networks for Pattern Recognition*. Oxford University PressOxford.

Bryliński, Ł., Brylińska, K., Woliński, F., Sado, J., Smyk, M., Komar, O., Karpiński, R., Prządka, M., & Baj, J. (2025). Trace Elements—Role in Joint Function and Impact on Joint Diseases. *International Journal of Molecular Sciences*, *26*(15), 7493. https://doi.org/10.3390/ijms26157493

Cai, S., Yang, S., Zheng, F., Lu, M., Wu, Y., & Krishnan, S. (2013). Knee joint vibration signal analysis with matching pursuit decomposition and dynamic weighted classifier fusion. *Computational and Mathematical Methods in Medicine*, *2013*(1), 904267. https://doi.org/10.1155/2013/904267

Castro Mejia, A., Gulde, P., & González Salinas, C. (2024). A clinical application of gait quality patterns in osteoarthritis. *Gait & Posture*, *114*, 284–289. https://doi.org/10.1016/j.gaitpost.2024.10.011

Cortes, C., & Vapnik, V. (1995). Support-vector networks. *Machine Learning*, *20*, 273–297. https://doi.org/10.1007/BF00994018

Courties, A., Kouki, I., Soliman, N., Mathieu, S., & Sellam, J. (2024). Osteoarthritis year in review 2024: Epidemiology and therapy. *Osteoarthritis and Cartilage*, *32*(11), 1397–1404. https://doi.org/10.1016/j.joca.2024.07.014

Cover, T., & Hart, P. (1967). Nearest neighbor pattern classification. *IEEE Transactions on Information Theory*, *13*(1), 21–27. https://doi.org/10.1109/TIT.1967.1053964

De Tocqueville, S., Marjin, M., & Ruzek, M. (2021). A review of the vibration arthrography technique applied to the knee diagnostics. *Applied Sciences*, *11*(16), 7337. https://doi.org/10.3390/app11167337

Diamond, L. E., Grant, T., & Uhlrich, S. D. (2024). Osteoarthritis year in review 2023: Biomechanics. *Osteoarthritis and Cartilage*, *32*(2), 138–147. https://doi.org/10.1016/j.joca.2023.11.015

Falkowicz, K., & Kulisz, M. (2024). Prediction of buckling behaviour of composite plate element using artificial neural networks. *Advances in Science and Technology Research Journal*, *18*(1), 231–243. https://doi.org/10.12913/22998624/177399

Gelber, A. C. (2024). Knee osteoarthritis. *Annals of Internal Medicine*, *177*(9), ITC129–ITC144. https://doi.org/10.7326/ANNALS-24-01249

Goodfellow, I., Courville, A., & Bengio, Y. (2016). *Deep learning*. The MIT Press.

Hosmer, D. W., Lemeshow, S., & Sturdivant, R. X. (2013). *Applied Logistic Regression* (1st ed.). John Wiley & Sons.

Jedliński, Ł., & Jonak, J. (2017). A disassembly-free method for evaluation of spiral bevel gear assembly. *Mechanical Systems and Signal Processing*, *88*, 399–412. https://doi.org/10.1016/j.ymssp.2016.11.005

Jedliński, Ł., Syta, A., Gajewski, J., & Jonak, J. (2022). Nonlinear analysis of cylindrical gear dynamics under varying tooth breakage. *Measurement*, *190*, 110721. https://doi.org/10.1016/j.measurement.2022.110721

Karpiński, R. (2022). Knee joint osteoarthritis diagnosis based on selected acoustic signal discriminants using machine learning. *Applied Computer Science*, *18*(2), 71–85. https://doi.org/10.35784/acs-2022-14

Karpiński, R., Prus, A., Baj, J., Radej, S., Prządka, M., Krakowski, P., & Jonak, K. (2025a). Articular cartilage: Structure, biomechanics, and the potential of conventional and advanced diagnostics. *Applied Sciences*, *15*(12), 6896. https://doi.org/10.3390/app15126896

Karpiński, R., Prus, A., Jonak, K., & Krakowski, P. (2025b). Vibroarthrography as a noninvasive screening method for early diagnosis of knee osteoarthritis: A review of current research. *Applied Sciences*, *15*(1), 279. https://doi.org/10.3390/app15010279

Karpiński, R., Szabelski, J., Krakowski, P., Jonak, J., Falkowicz, K., Jojczuk, M., Nogalski, A., & Przekora, A. (2024a). Effect of various admixtures on selected mechanical properties of medium viscosity bone cements: Part 1 – α/β tricalcium phosphate (TCP). *Composite Structures*, *343*, 118306. https://doi.org/10.1016/j.compstruct.2024.118306

Karpiński, R., Szabelski, J., Krakowski, P., Jonak, J., Falkowicz, K., Jojczuk, M., Nogalski, A., & Przekora, A. (2024b). Effect of various admixtures on selected mechanical properties of medium viscosity bone cements: Part 2 – Hydroxyapatite. *Composite Structures*, *343*, 118308. https://doi.org/10.1016/j.compstruct.2024.118308

Karpiński, R., Szabelski, J., Krakowski, P., Jonak, J., Falkowicz, K., Jojczuk, M., Nogalski, A., & Przekora, A. (2024c). Effect of various admixtures on selected mechanical properties of medium viscosity bone cements: Part 3 – Glassy carbon. *Composite Structures*, *343*, 118307. https://doi.org/10.1016/j.compstruct.2024.118307

Khokhlova, L., Komaris, D.-S., Tedesco, S., & O'Flynn, B. (2021). Assessment of hip and knee joints and implants using acoustic emission monitoring: A scoping review. *IEEE Sensors Journal*, *21*(13), 14379–14388. https://doi.org/10.1109/JSEN.2020.3045203

Kohn, M. D., Sassoon, A. A., & Fernando, N. D. (2016). Classifications in brief: kellgren-lawrence classification of osteoarthritis. *Clinical Orthopaedics & Related Research*, *474*(8), 1886–1893. https://doi.org/10.1007/s11999-016-4732-4

Krakowski, P., Karpiński, R., Jonak, J., & Maciejewski, R. (2021). Evaluation of diagnostic accuracy of physical examination and MRI for ligament and meniscus injuries. *Journal of Physics: Conference Series*, *1736*, 012027. https://doi.org/10.1088/1742-6596/1736/1/012027

Kręcisz, K. (2023). Correlation between linear and non-linear vibroartrographic parameters. *Przegląd Elektrotechniczny*, *1*(7), 182–187. https://doi.org/10.15199/48.2023.07.33

Kulisz, M., Kłosowski, G., Rymarczyk, T., Hoła, A., Niderla, K., & Sikora, J. (2024). The use of the multi-sequential LSTM in electrical tomography for masonry wall moisture detection. *Measurement*, *234*, 114860. https://doi.org/10.1016/j.measurement.2024.114860

Kulisz, M., Kłosowski, G., Rymarczyk, T., Słoniec, J., Gauda, K., & Cwynar, W. (2024). Optimizing the neural network loss function in electrical tomography to increase energy efficiency in industrial reactors. *Energies*, *17*(3), 681. https://doi.org/10.3390/en17030681

Kulisz, M., Kujawska, J., Cioch, M., Cel, W., & Pizoń, J. (2024). Comparative analysis of machine learning methods for predicting energy recovery from waste. *Applied Sciences*, *14*(7), 2997. https://doi.org/10.3390/app14072997

Kwiatkowski, A., Sobolewski, O., Wyłomańska, A., Sawicki, M., Zieleń, P., Druszcz, A., & Ptak, M. (2023). Development of artificial intelligence algorithms to analyse weather conditions for the prediction of cerebrovascular accidents. In H. Podbielska & M. Kapalla (Eds.), *Predictive, Preventive, and Personalised Medicine: From Bench to Bedside* (Vol. 17, pp. 283–304). Springer International Publishing. https://doi.org/10.1007/978-3-031-34884-6_16

Litak, G., Syta, A., Gajewski, J., & Jonak, J. (2010). Detecting and identifying non-stationary courses in the ripping head power consumption by recurrence plots. *Meccanica*, *45*(4), 603–608. https://doi.org/10.1007/s11012-009-9265-4

Łysiak, A., Bączkowicz, D., Borzucka, D., Szmajda, M., Kawala-Sterniuk, A., Brol, S., Dołęgowski, M., & Mroczka, J. (2025). Regression analysis of the vibroarthrogram in the external load conditions. *Advances in Science and Technology Research Journal*, *19*(10), 238–251. https://doi.org/10.12913/22998624/207975

Machrowska, A., Karpiński, R., Jonak, J., Szabelski, J., & Krakowski, P. (2020a). Numerical prediction of the component-ratio-dependent compressive strength of bone cement. *Applied Computer Science*, *16*(3), 88–101. https://doi.org/10.23743/acs-2020-24

Machrowska, A., Karpiński, R., Maciejewski, M., Jonak, J., & Krakowski, P. (2024a). Application of EEMD-DFA algorithms and ann classification for detection of knee osteoarthritis using vibroarthrography. *Applied Computer Science*, *20*(2), 90–108. https://doi.org/10.35784/acs-2024-18

Machrowska, A., Karpiński, R., Maciejewski, M., Jonak, J., Krakowski, P., & Syta, A. (2024b). Application of recurrence quantification analysis in the detection of osteoarthritis of the knee with the use of vibroarthrography. *Advances in Science and Technology Research Journal*, *18*(5), 19–31. https://doi.org/10.12913/22998624/189512

Machrowska, A., Karpiński, R., Maciejewski, M., Jonak, J., Krakowski, P., & Syta, A. (2025). Multi-scale analysis of knee joint acoustic signals for cartilage degeneration assessment. *Sensors*, *25*(3), 706. https://doi.org/10.3390/s25030706

Machrowska, A., Szabelski, J., Karpiński, R., Krakowski, P., Jonak, J., & Jonak, K. (2020b). Use of deep learning networks and statistical modeling to predict changes in mechanical parameters of contaminated bone cements. *Materials*, *13*(23), 5419. https://doi.org/10.3390/ma13235419

Matthews, E., Waterson, H. B., Phillips, J. R., & Toms, A. D. (2020). Zonal fixation in knee replacement surgery – is there any clinical or biomechanical evidence to justify it? *Bone & Joint 360*, *9*(5), 4–9. https://doi.org/10.1302/2048-0105.95.360801

McPherson, A., McDaid, A. J., & Ward, S. (2024). Toward personalized orthopedic care: Validation of a smart knee brace. *Digital Biomarkers*, *8*(1), 75–82. https://doi.org/10.1159/000538487

Messaoudene, K., & Harrar, K. (2022). A hybrid LBP-HOG model and naive bayes classifier for knee osteoarthritis detection: Data from the osteoarthritis initiative. In B. Lejdel, E. Clementini, & L. Alarabi (Eds.), *Artificial Intelligence and Its Applications* (Vol. 413, pp. 458–467). Springer International Publishing. https://doi.org/10.1007/978-3-030-96311-8_42

Mitchell, T. M. (2013). *Machine learning* (Nachdr.). McGraw-Hill.

Mohammadi, S., Salehi, M. A., Jahanshahi, A., Shahrabi Farahani, M., Zakavi, S. S., Behrouzieh, S., Gouravani, M., & Guermazi, A. (2024). Artificial intelligence in osteoarthritis detection: A systematic review and meta-analysis. *Osteoarthritis and Cartilage*, *32*(3), 241–253. https://doi.org/10.1016/j.joca.2023.09.011

Olsson, S., Akbarian, E., Lind, A., Razavian, A. S., & Gordon, M. (2021). Automating classification of osteoarthritis according to Kellgren-Lawrence in the knee using deep learning in an unfiltered adult population. *BMC Musculoskeletal Disorders*, *22*, 844. https://doi.org/10.1186/s12891-021-04722-7

Rangayyan, R. M., Krishnan, S., Bell, G. D., Frank, C. B., & Ladly, K. O. (1997). Parametric representation and screening of knee joint vibroarthrographic signals. *IEEE Transactions on Biomedical Engineering*, *44*(11), 1068–1074. https://doi.org/10.1109/10.641334

Rangayyan, R. M., & Wu, Y. (2009). Analysis of vibroarthrographic signals with features related to signal variability and radial-basis functions. *Annals of Biomedical Engineering*, *37*(1), 156–163. https://doi.org/10.1007/s10439-008-9601-1

Sbriglio, C., Ptak, M., Dymek, M., Sawicki, M., & Kwiatkowski, A. (2025). Modelling and analysis of cerebrospinal fluid flow in the human brain – Is cerebrospinal fluid an effective protective mechanism during high-impact loading? *Acta of Bioengineering and Biomechanics*, *27*(1). https://doi.org/10.37190/ABB-02591-2025-02

Shark, L.-K., Chen, H., & Goodacre, J. (2011). Knee acoustic emission: A potential biomarker for quantitative assessment of joint ageing and degeneration. *Medical Engineering & Physics*, *33*(5), 534–545. https://doi.org/10.1016/j.medengphy.2010.12.009

Slattery, C., & Kweon, C. Y. (2018). Classifications in brief: Outerbridge classification of chondral lesions. *Clinical Orthopaedics & Related Research*, *476*(10), 2101–2104. https://doi.org/10.1007/s11999.0000000000000255

Steinmetz, J. D., Culbreth, G. T., Haile, L. M., Rafferty, Q., Lo, J., Fukutaki, K. G., Cruz, J. A., Smith, A. E., Vollset, S. E., Brooks, P. M., Cross, M., Woolf, A. D., Hagins, H., Abbasi-Kangevari, M., Abedi, A., Ackerman, I. N., Amu, H., Antony, B., Arabloo, J., … Kopec, J. A. (2023). Global, regional, and national burden of osteoarthritis, 1990–2020 and projections to 2050: A systematic analysis for the Global Burden of Disease Study 2021. *The Lancet Rheumatology*, *5*(9), e508–e522. https://doi.org/10.1016/S2665-9913(23)00163-7

Szabelski, J., Karpiński, R., & Machrowska, A. (2022). Application of an artificial neural network in the modelling of heat curing effects on the strength of adhesive joints at elevated temperature with imprecise adhesive mix ratios. *Materials*, *15*(3), 721. https://doi.org/10.3390/ma15030721

Tanaka, N., & Hoshiyama, M. (2012). Vibroarthrography in patients with knee arthropathy. *Journal of Back and Musculoskeletal Rehabilitation*, *25*(2), 117–122. https://doi.org/10.3233/BMR-2012-0319

Wang, Y., Zheng, T., Song, J., & Gao, W. (2021). A novel automatic Knee Osteoarthritis detection method based on vibroarthrographic signals. *Biomedical Signal Processing and Control*, *68*, 102796. https://doi.org/10.1016/j.bspc.2021.102796

Whittingslow, Daniel. C., Jeong, H.-K., Ganti, V. G., Kirkpatrick, N. J., Kogler, G. F., & Inan, O. T. (2020). Acoustic emissions as a non-invasive biomarker of the structural health of the knee. *Annals of Biomedical Engineering*, *48*, 225–235. https://doi.org/10.1007/s10439-019-02333-x

Wipperman, M. F., Lin, A. Z., Gayvert, K. M., Lahner, B., Somersan-Karakaya, S., Wu, X., Im, J., Lee, M., Koyani, B., Setliff, I., Thakur, M., Duan, D., Breazna, A., Wang, F., Lim, W. K., Halasz, G., Urbanek, J., Patel, Y., Atwal, G. S., … Harari, O. (2024). Digital wearable insole-based identification of knee arthropathies and gait signatures using machine learning. *eLife*, *13*, e86132. https://doi.org/10.7554/eLife.86132

Wu, Y., Chen, P., Luo, X., Huang, H., Liao, L., Yao, Y., Wu, M., & Rangayyan, R. M. (2016). Quantification of knee vibroarthrographic signal irregularity associated with patellofemoral joint cartilage pathology based on entropy and envelope amplitude measures. *Computer Methods and Programs in Biomedicine*, *130*, 1–12. https://doi.org/10.1016/j.cmpb.2016.03.021

Zalzal, P., Papini, M., Petruccelli, D., De Beer, J., & Winemaker, M. J. (2004). An in vivo biomechanical analysis of the soft-tissue envelope of osteoarthritic knees. *The Journal of Arthroplasty*, *19*(2), 217–223. https://doi.org/10.1016/j.arth.2003.09.008